Tuning the antimicrobial behaviour of Cu85Zr15 thin films in "wet" and "dry" conditions through structural modifications

Victor M. Villapún, C.C. Lukose, M. Birkett, L.G. Dover, S. González

PII: S0257-8972(18)30695-9
DOI: doi:10.1016/j.surfcoat.2018.06.094
Reference: SCT 23572

To appear in: *Surface & Coatings Technology*

Received date: 4 April 2018
Revised date: 12 June 2018
Accepted date: 30 June 2018

Please cite this article as: Victor M. Villapún, C.C. Lukose, M. Birkett, L.G. Dover, S. González , Tuning the antimicrobial behaviour of Cu85Zr15 thin films in "wet" and "dry" conditions through structural modifications. Sct (2018), doi:10.1016/j.surfcoat.2018.06.094

Tuning the antimicrobial behaviour of $Cu_{85}Zr_{15}$ thin films in "wet" and "dry" conditions through structural modifications

Victor M. Villapún[a], C.C. Lukose [a], M. Birkett [a], L.G. Dover[b], S. González[a,*]

[a]Faculty of Engineering and Environment, Northumbria University, Newcastle upon Tyne NE1 8ST, UK
[b]Faculty of Health and Life Sciences, Northumbria University, Newcastle upon Tyne NE1 8ST, UK

Abstract:

The antimicrobial behaviour of $Cu_{85}Zr_{15}$ at. % thin films prepared by magnetron sputtering was studied in both wet and dry conditions. Small variations in key deposition processing parameters (pressure and substrate temperature) enabled the growth of thin films with similar nanostructures but different degrees of compactness, according to the Thornton's structural zone model. This model has proven its effectiveness in providing sensitive structural information to explain significant differences in antimicrobial behaviour of the CuZr thin films, even when processing conditions lie within the same structural zone. The antimicrobial behaviour has been studied for *E. coli* and *S. aureus* for up to 4 hours of "dry" contact. Structures of lower compactness, grown at higher deposition pressure, are shown to provide higher antimicrobial activity for "dry" conditions than for "wet" conditions. For thin films of CuZr deposited at 0.5 Pa, the reduction percentage of bacteria is 99.47 %, which is much higher than the results of 70-80 % obtained for the films deposited at 0.1 and 0.3 Pa. Microscopy studies indicate that for 4 hours of contact time, bacteria exhibit inner damage and even lysis, however, no morphological changes are detected because of the short timeframes used.

Keywords: Antimicrobial properties; Thornton's model; Thin film; Magnetron sputtering; Processing conditions

*Corresponding author. Tel.: +44 (0) 191 349 5937
E-mail address: sergio.sanchez@northumbria.ac.uk (S. González)

1. Introduction

Over the years, many authors have studied the antimicrobial behaviour of copper (Cu), Zinc (Zn) and silver (Ag) and their alloys because they can kill a broad spectrum of bacteria. The first papers about the biocidal properties of metallic thin films were focused on the addition of Ag, while those dealing with the antimicrobial properties of Cu were relatively scarce [1, 2]. The antimicrobial behaviour of Ag-containing thin films [3] is attributed to the interaction of Ag ions with the thiol groups of bacteria proteins, affecting the replication of DNA, uncoupling the respiratory chain from oxidative phosphorylation or collapsing the proton motive force across the cytoplasmic membrane [4]. The antimicrobial properties of this element are highly temperature and humidity dependent, optimally at 35°C and 95 % RH, respectively [5] and are considered to be caused by silver oxide rather than pure silver [6-8].

However, in comparison, copper can kill bacteria across all levels of temperature and humidity [5] and its outstanding biocidal performance is associated to the liberation of Cu^{+1} and Cu^{+2} ions [9-11] as observed in alloy systems such as Cu-Zr-Ag [3] and Cu-Ti [12]. Most of the reported antimicrobial studies have been carried out on fully crystalline copper and copper based alloys, while the antimicrobial activity of these materials with amorphous/nanocrystalline structures obtained by rapid solidification techniques (i.e., magnetron sputtering) has been mostly overlooked. This is remarkable since these material structures are known to display very interesting properties such as higher strength, lower elastic modulus and superior corrosion resistance compared to their crystalline counterparts [13, 14]. Some recent examples of the latter are Cu-Zr thin films that exhibit antimicrobial activity even for low Cu concentrations [15]. Even for copper concentrations as low as 30 at. %, such as in $(Zr_{55}Al_{10}Ni_5Cu_{30})_{100-x}Y_x$ (x= 0 or 1 at. %) alloys, the number of *S. aureus* was significantly reduced after 4 h of contact compared to the Ti-6Al-4V control [16]. As could be expected, increasing the concentration of Cu in the alloy increases the killing efficiency (i.e., less time to kill bacteria) [17] of bacteria attached to the alloy.

There are several methods for the production of such nanostructured thin films, such as electroless plating [18], but physical vapour deposition (PVD) is perhaps the most widely used. Among the PVD processes, magnetron sputtering is especially relevant due to its ability to accurately ~~the high deposition rates and widely~~ control the microstructure and composition of the growing thin film [19, 20] by fine tuning various key process parameters such as the substrate temperature and sputtering pressure. The microstructure of the thin film also depends on its chemical composition since the glass forming ability is composition-dependent. For example, co-sputtered binary Zr_xCu_{100-x} thin films [21] containing more than 80 at. % Zr or Cu are crystalline while for intermediate compositions they exhibit a low order phase (i.e., amorphous) according to both experimental results and molecular dynamic simulations. Among all the amorphous thin films, the one with highest copper content reported until now is $Zr_{20}Cu_{80}$ at. % and there is no experimental information whether thin films of higher Cu concentrations (between 80 and 97 at. %) are amorphous or crystalline. Moreover, the antimicrobial activity of such alloys has not been studied despite their potential interest attributed to the high copper content.

There are several methods to quantify the antimicrobial activity of surfaces in the literature [22] that are similar to those observed in catheters or drainages, but these are “wet” test conditions, where the liquid phase in the broth media is always present. While for applications such as touch surfaces the conditions are always “dry”. Consequently, some authors have begun to investigate this issue, encouraging the development of “dry” tests, where the media is completely evaporated [23-25]. However, the influence of air-drying on

the morphology of *E. coli* and *S. aureus* is still not completely understood [26, 27]. As previously mentioned, the antimicrobial activity may depend on the environmental conditions, and, it is of interest to explore the possibility of tuning the processing conditions of magnetron sputtering to control the antimicrobial performance. For this reason, this manuscript aims to shed light on the effect of varying the magnetron sputtering processing conditions of pressure and substrate temperature on the antimicrobial performance of Cu_{85}-Zr_{15} thin film evaluated when the liquid phase in the LB media is always present (considered as "wet" conditions), in contrast to samples where the media completely evaporated (denominated as "dry" tests).

2. Methods

2.1. Thin film fabrication

Thin films were prepared by the magnetron sputtering technique using a Teer Coatings UDP multi-cathode deposition plant. Substrates of 314 stainless steel (314SS) (5 x 5 x 1 mm thick) with a surface roughness, Ra<0.5 µm and soda lime glass slides (25.4 x 76.2 x 1mm thick) were used. Before deposition all substrates were thoroughly cleaned in 1:5 ratio of DECON90 solution to water for 60 seconds, rinsed in deionised water and dried with a nitrogen blast to clean off residues and particles before being loaded on a rotating carousel in the centre of the deposition chamber. The chamber was then evacuated to a base pressure of $5x10^{-4}$ Pa before pure argon was introduced at the required flow rate to control the working pressure. A rectangular copper (Cu) target (248 x 133 x 10 mm thick) and circular zirconium (Zr) target (100 mm dia. X 3 mm thick), both of 99.99 % purity, were then sputtered cleaned at dc powers of 200 W and 160 W respectively for 10 min. Following cleaning, the cathode shutters were opened and the Cu and Zr targets were co-sputtered for 90 min onto the substrates mounted at a distance of 130 mm from the targets on the central carousel, which was rotated at a fixed speed of 5 rpm. These deposition conditions resulted in thin films of approximate chemical composition Cu/Zr 85/15 at. % and 1 µm in thickness. In total four different batches of Cu-Zr films were deposited; three at room temperature and varying working pressures of 0.1, 0.3 and 0.5 Pa and an additional batch at a substrate temperature of 403K and working pressure of 0.3 Pa. Full details of the deposition conditions for these four batches are given in Table 1.

Table 1 Cu-Zr thin film deposition conditions

Batch	Base	Ar	Working	Substrate	Cathode power (W)

ID	pressure (Pa)	flowrate (sccm)	pressure (Pa)	temperature (K)	Cu	Zr
1RT	$5x10^{-4}$	10	0.1	R_T	200	160
3RT	$5x10^{-4}$	30	0.3	R_T	200	160
5RT	$5x10^{-4}$	45	0.5	R_T	200	160
3HT	$5x10^{-4}$	30	0.3	403	200	160

2.2. Structural and physical properties of thin films

The surface morphology and chemical composition of the Cu-Zr film samples sputtered on to 314SS substrates and borosilicate glass slides were analysed using a Tescan Mira 3, Scanning Electron Microscope (SEM) with 5-10 kV of acceleration voltage, coupled with an Oxford Instruments X-Max 150 Energy Dispersive X-ray (EDX) detector. The surface topography and roughness of the films was analysed and measured using a Digital instrument DimensionsTM 3100 atomic force microscope (AFM) system scanning in contact mode across a 3 x 3 μm^2 sample area; data was visualised using Gwyddion software and processed in MATLAB software suite. The structural properties of the films were determined from X-ray diffraction (XRD) patterns collected using a Siemens D5000 diffractometer with Cu Kα radiation (λ = 1.54184 Å) at 40 kV and 40 mA, with a scanning speed of 0.01°/s in the 2θ range 10° to 90°.

Film thickness was measure using a Dekatak XTL stylus type profilemeter equipped with a 12.5 µm tip. A square edge step was created in the films grown on glass slides using a strip of 3 mm wide Kapton tape, which was removed after deposition.

Contact angle measurements were carried out using the sessile drop technique (Krüss drop size DSA30 analyser). A volume of 1 µL of deionised water was deposited at a rate of 30 µL/min on the surface of the samples, and the angle was immediately observed to prevent droplet shape change due to evaporation. Contact angle results are the average of five sessile drop tests (ten contact angle measurements).

2.3. Antimicrobial behaviour of thin films

The antibacterial activity of the thin films was assessed by following the reduction in colony forming units (CFU) recovered from the surface of the thin films over contact time using *E. coli K12* (Gram-negative) and *S. aureus* NCTC 6571 (Gram-positive) [28]. For the antimicrobial tests, bacteria were cultured in an orbital incubator (37°C, 200 rpm), in 25 mL of LB (Luria Bertani) broth for 16 h. Culture yield was quantified by measuring optical density and bacteria were then diluted in sterile LB Broth to an optical density (OD_{600}) of 0.01. The diluted cultures were incubated at 37°C until they reached an OD_{600} ~ 0.3; approx. $3x10^8$ per

mL. Thin films and control samples (bare 314SS) were immersed in pure ethanol and sonicated for 5 min to ensure a clean and disinfected surface. A quantity of 2 µL of the culture was dispensed directly onto the test surfaces. For the wet tests, these samples were placed inside a sterile petri dish containing tissue paper wetted with 1 mL of sterile LB Broth to prevent sample drying. For the dry tests, all samples were placed inside petri dishes, but no wetted tissue was added. To ensure complete drying, after inoculation, the petri dishes were placed 100 mm away from a Bunsen burner with the lid partially open. After the inoculum vehicle evaporated completely (around 8-9 min), all petri dishes were closed and left on a bench at room temperature. After the designated exposure time, the “wet” and “dry” samples were diluted in 198 µL of Tween 20 0.148 g/L (2 × CMC) and sonicated for 5 min. Finally, the recovered bacterial suspension was subjected to serial decimal dilution, spread onto LB agar plates and the resulting colonies were counted after 16 h of incubation at 37°C. All tests were performed five times, with mean counts and standard deviation reported.

2.4. Morphological characterization of bacteria

The morphology of the bacteria was analysed from Scanning Electron Microscopy (SEM) and Transmission Electron Microscopy (TEM).

SEM images of deposited bacteria in “dry” and “wet” conditions were collected using a variation of the method described by Fisher et al. [29]. Inoculum preparation and disinfection of the samples was done as previously described for the antibacterial tests in section 2.3. 2 µL of inoculum was deposited on the samples and left for up to 4 h at room temperature (i.e., the bacteria-surface contact time for this work) in a sterile petri dish with a wetted cloth with 1 mL of LB broth, for the wet conditions, and without it in the dry conditions. Each sample was transferred to a 24 well tissue culture plate (circular well diameter 15mm) and 1 mL of 2.5 % glutaraldehyde was added gently against the wall of the well to limit disruption of surface attachment. After 1 h, samples were washed with phosphate-buffered saline (PBS) three times for 2 min each. Fixed samples were dehydrated using an ethanol/water series (25 %, 50 %, 75 % and 95 % v/v); samples were immersed in 1 mL of each ethanol dilution for 5 min, and 10 min in pure ethanol. After drying, samples were coated with platinum (2-3 nm) using a Q150R Rotary-Pumped Sputter Coater (Quorum Technologies).

TEM images of *E. coli* and *S. aureus* cells deposited in “dry” conditions on the 5RT thin film sample after 4 h, were taken with a Philips Cm 100 Compustage (FEI) TEM, while digital images were collected using an AMT CCD camera (Deben). Inoculation and recovery was carried out as described in the antimicrobial methods in section 2.3. After 5 min of sonication in 198 µL of Tween 20, samples were centrifuged at 5000 x g until a pellet was visible. Supernatant (Tween 20) was removed by pipetting without disturbing the pellet and cells

were re-suspended in 2 % glutaraldehyde in sodium cacodylate buffer (4°C) for 1 h. In the following steps, samples were centrifuged at 3000 rpm in 5 min cycles until a pellet was visible in the bottom of the microcentrifuge tubes. Cells were rinsed in cacodylate buffer twice for 10 min each, followed by a secondary fixation in 1% osmium tetroxide in deionised water for 30 min. Samples were washed in deionised water twice for 10 min and subjected to dehydration through a serial dilution of acetone in dH_2O (25 %, 50 %, 75 % for 15 min each) and twice in pure acetone for 20 min each. All samples were impregnated with 25 %, 50 %, 75 % resin (TAAB epoxy resin) in acetone (30 min) and 100 % resin for a minimum of 3 changes over 24 h. After the impregnation, microcentrifuge tubes were filled with 100% fresh resin, re-suspended and polymerised at 60°C for 24 h. Once complete polymerisation was achieved, 0.5 µm sections were cut and stained with 1 % toluidine blue in 1% borax. Ultrathin sections (~70 nm) were obtained using a diamond knife on a RMC MT-XL ultramicrotome. Sections were stretched with chloroform to eliminate compression and mounted on Pioloform-filmed copper grids.

2.5. Copper ion diffusion

To measure the number of copper ions released from our samples, 2 µL of LB broth were deposited on the 1RT and 5RT samples. All samples were disinfected and degreased using the same protocol described in the antimicrobial test (section 2.3), and placed into a sterile petri dish with a wetted cloth for “wet” tests, and without for “dry” tests. After 1 and 4 h of contact time, samples were introduced into a cleaned and disinfected universal bottle containing 2.0 mL of deionized water from a Mil-li-DI purification system. Samples were sonicated for 5 min and MGs were subsequently recovered. Dilutions were processed using Inductively Coupled Plasma spectrometry (PerkinElmer Optima 8000 ICP-OES). All tests were carried out three times with mean counts and standard deviation reported.

3. Results and discussion

3.1. Structural and physiochemical properties

Thin films were produced by magnetron sputtering under a variety of conditions with regards to substrate temperature and working pressure. The chemical composition of the Cu-Zr films grown on 314SS as well as the film thickness on both 314SS and glass substrates are reported in Table 2. The composition was measured by EDX in the SEM.

Table 2 Chemical composition and thickness of the Cu-Zr thin films. All results are based on the measurement of 5 film samples from each batch.

Batch ID	Composition (at.%)		Film thickness (µm)	
	Cu	Zr	Glass	314SS
1RT	84.1 ± 0.2	15.9 ± 0.2	1.02 ± 0.02	1.12 ± 0.04
3RT	84.7 ± 0.1	15.3 ± 0.1	1.10 ± 0.06	1.07 ± 0.05
5RT	85.7 ± 0.2	14.4 ± 0.2	1.06 ± 0.06	1.19 ± 0.13
3HT	84.6 ± 0.1	15.4 ± 0.1	1.17 ± 0.10	1.33 ± 0.05

The chemical composition of the films was found to be consistently close to the target of Cu/Zr 85/15 at. % for all samples and the distribution Cu and Zr in the film was found to be homogeneous with no noticeable agglomeration. There was a slight increase in Cu concentration of around 1.5 at. % with increase in sputtering pressure, from a mean value of 84.1 at. % for films deposited at 0.1 Pa (1RT) to 85.7 at. % for those deposited at 0.5 Pa (5RT). This slight increase can be related to variation in sputter yield of the two target elements with increase in deposition pressure [30]. The difference in composition is similar to the accuracy of the technique and therefore can be regarded as identical. No significant difference in composition was measured for the films deposited at 0.3 Pa with and without substrate heating (3HT and 3RT). The mean thickness of the films deposited on both 314SS and glass substrates ranges from 1.02 to 1.33 µm, with no significant difference observed for films deposited at different pressures or substrate temperatures.

Figure 1 shows SEM micrographs from the cross-section and from the surface of the Cu-Zr thin films deposited at varying sputtering pressures. The surface of the films shows fine grains of up to about 100 µtypical of nanocrystalline/amorphous structures, which are frequently observed when sputtering multi-component materials due to the reduction in grain boundary scattering [31, 32]. At the same time, some nodular growth flaws (see arrows) caused by imperfections on the substrate (SS314) can be noticed. There is a slight coarsening of the grains and the development of a more columnar semi-crystalline structure with increase in sputtering pressure to 0.3 Pa (3RT) and a slightly more porous surface morphology for the films deposited at 0.5 Pa (5RT). The development of this columnar structure is also apparent for the films grown with substrate heating at 0.3 Pa (3HT); however, the surface of these films exhibited a more fibrous texture due to the elevated substrate temperature during deposition [33]. These observed changes in film structure can be adequately explained using Thornton's structural zone model (SZM) [34] depicted in Figure 2. In this model, an increase in sputtering gas pressure allows more Ar adatoms to be

adsorbed at the substrate surface. This limits the mobility and hence the surface diffusion of arriving atoms resulting in a structure with porous grain boundaries. Conversely, an increase in substrate temperature enhances surface mobility and conventional bulk diffusion, producing a film structure consisting of more columnar grains with denser boundaries.

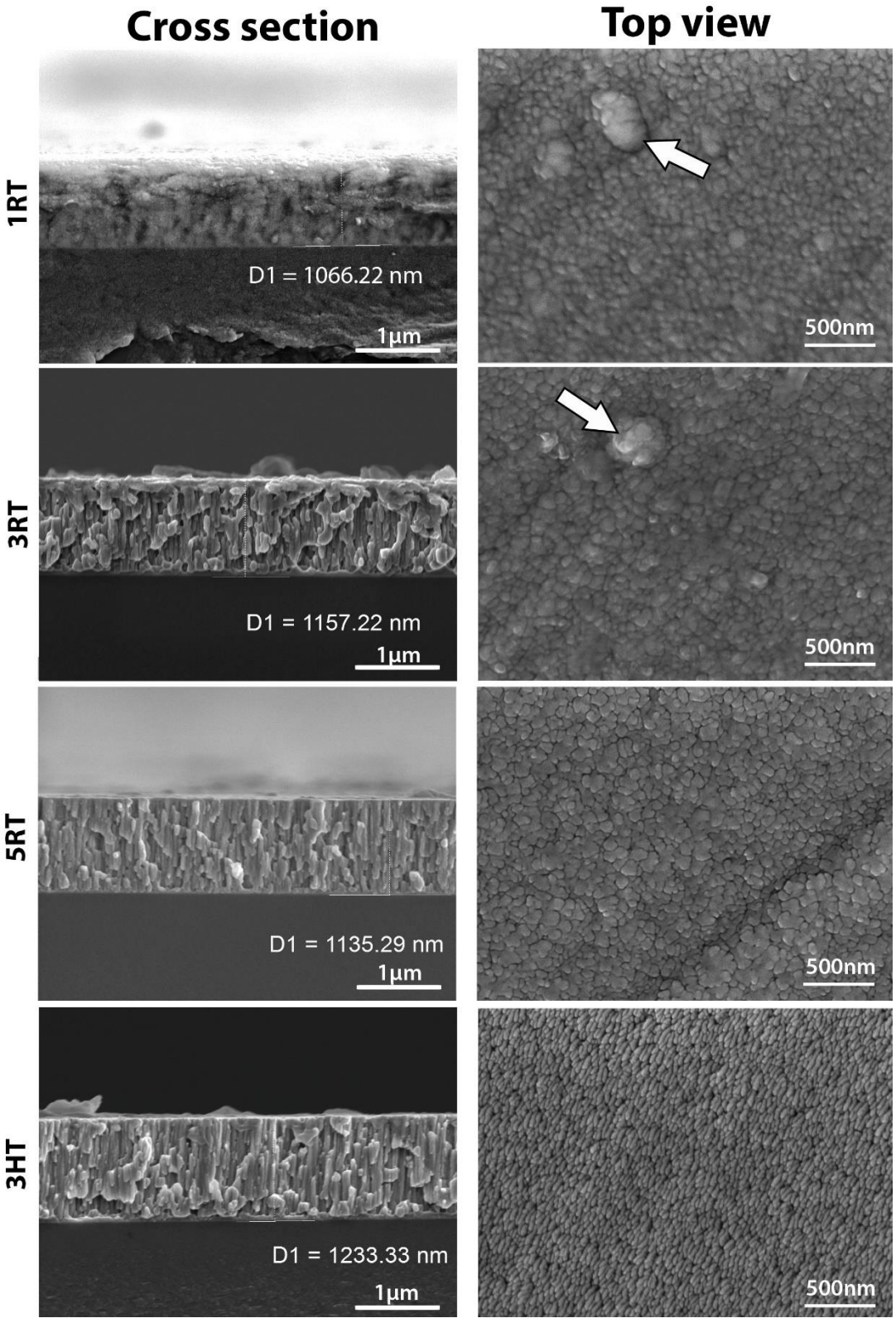

Figure 1 Secondary electron SEM images showing the cross section and the surface of the Cu-Zr thin films analysed.

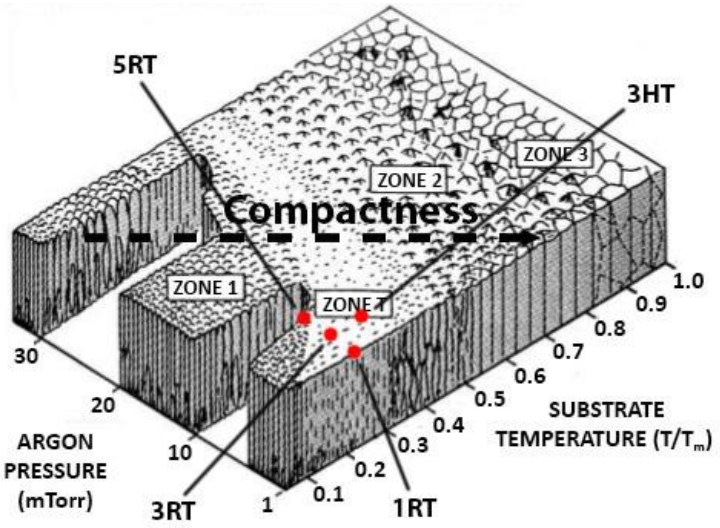

Figure 2 Thornton's structural zone model (SZM) of sputtered metallic thin films (T_m~1333K) [35]. Adapted from [36].

For the conditions used in our deposition set-up, the thin film prepared at the highest pressure at room temperature (5RT) will lie in Zone 1. This area of the Structure Zone Model (SZM) is characterized by tapered columnar grains separated by voids [37, 38], due to the preferential collection of incident atoms at protuberances in the substrate. A decrease in pressure with low substrate temperature (1RT) will change the structure to that of Zone T. This region is defined by a structure, which retains the columnar structure of Zone 1 but without the presence of voids, increasing the compactness of the thin film. In contrast, the films grown at the mid-range pressure of 0.3 Pa with and without substrate heating (3HT and 3RT) will lie in between Zones 1 and T, with the same structure as 5RT but with slightly more compactness [37, 38]. Consequently, variations in the structure of the films depicted in Figure 1 can be related to changes in pressure and substrate temperature during their deposition.

Figure 3 shows XRD spectra for the Cu-Zr thin films deposited on glass substrates at varying sputtering pressures and substrate temperature. All films exhibit a relatively broad halo peak of low intensity indicating a low ordered structure. These results are in good agreement with the film structures observed in the SEM images in Figure 1.

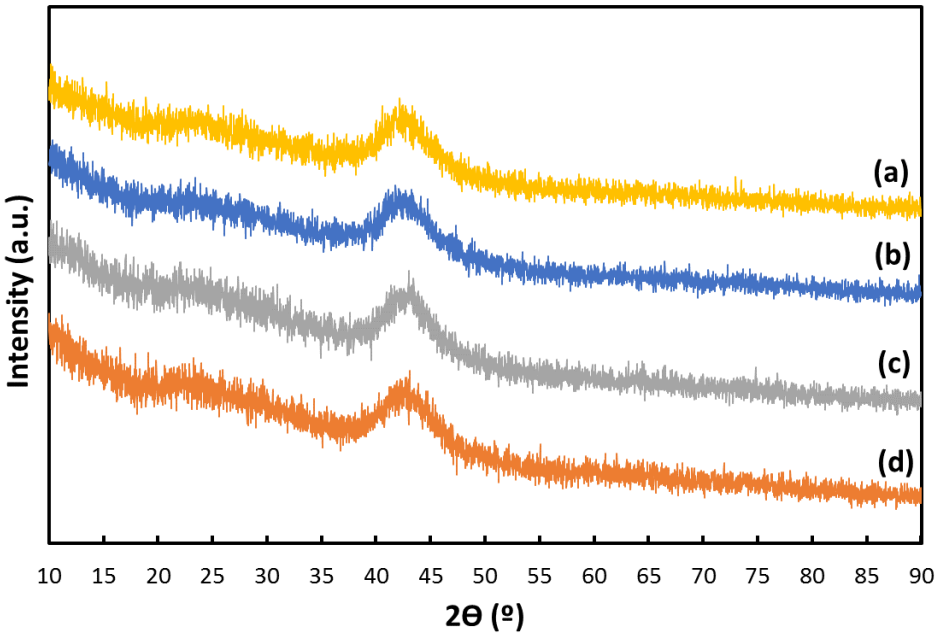

Figure 3 XRD patterns for the Cu-Zr thin films deposited at varying pressures (a) 1RT, (b) 3RT, (c) 5RT and (d) 3HT.

Considering that the deposition conditions have an effect on the structure and therefore on the surface roughness, the roughness values have been measured by AFM for the Cu-Zr thin films deposited on 314SS at varying sputtering pressures, are shown in Figure 4. The 3D images show crack-free surfaces consisting of grains of good repeatability for all samples. As sputtering pressure was increased from 0.1 (1RT) to 0.5 Pa (5RT), a slight coarsening of the grains and an increase in porosity was observed. Results for surface roughness measured from the AFM images are reported in Table 3. The ten-point mean roughness (R_z) showed a decrease in value from 26.39 to 20.79 nm with increase in sputtering pressure from 0.1 to 0.5 Pa, while the roughness average (R_a) value was in the range 4.97 to 6.02 nm for all film samples. A small increase in R_a to from 4.97 to 5.77 nm was observed for the films grown at 0.3 Pa with and without substrate heating (3HT and 3RT), which could be due to the development of the fibrous surface texture reported in the SEM image for the 3HT film in Figure 1.

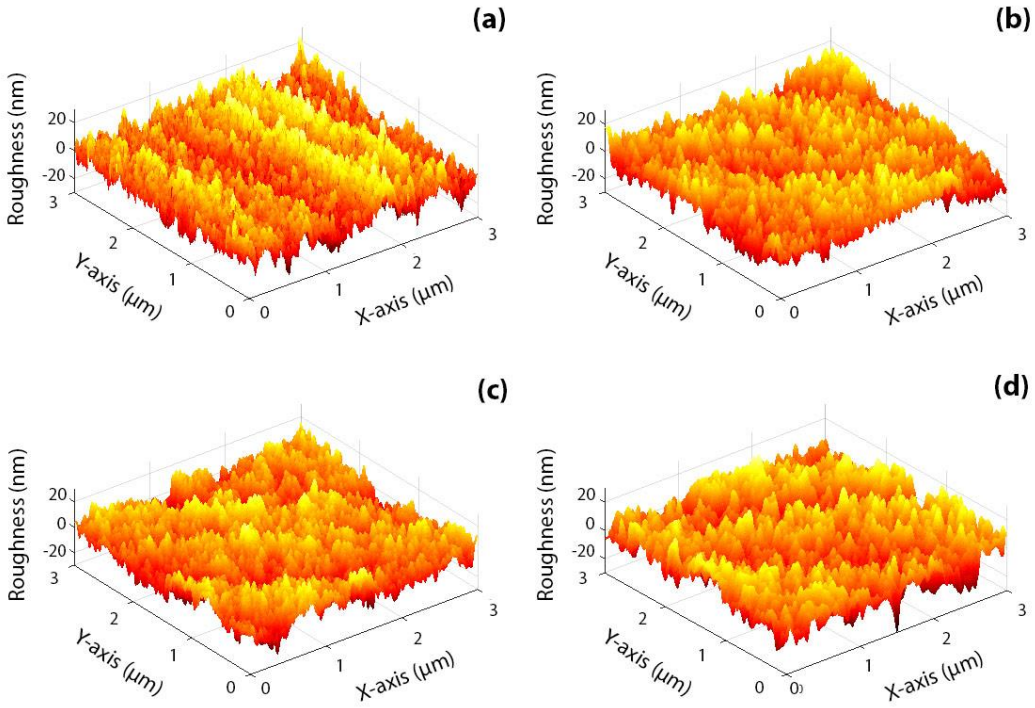

Figure 4 AFM images of the Cu-Zr thin films deposited on 314SS at varying pressures (a) 1RT, (b) 3RT, (c) 5RT and (d) 3HT.

Table 3. AFM roughness of the analysed thin films and of the uncoated steel substrate.

	314SS	
	R_a (nm)	R_z (nm)
Uncoated	3.49 ± 0.38	15.83 ± 2.94
1RT	6.02 ± 0.44	26.39 ± 3.33
3RT	4.97 ± 0.34	22.46 ± 2.90
5RT	5.33 ± 0.63	20.79 ± 2.24
3RT	5.77 ± 0.70	21.74 ± 2.03

3.2. Surface wettability

It is commonly accepted that the antimicrobial behaviour of copper is correlated to the diffusion of copper ions (i.e., Cu^{+1} and Cu^{+2}) into bacteria [39-41]. For antimicrobial touch surfaces this depends on the bacteria-surface contact area and therefore on the process which enables bacteria to adhere to surfaces. This process is complex and depends on numerous variables such as motility (i.e. ability to move actively), chemotaxis (i.e., ability to

move in relation to a concentration gradient for a specific chemical), as well as, physical features that directly promote adhesion such as flagella, glycocalyces or fimbriae. The sessile drop technique is known to be a simple and useful method to estimate the adhesion of bacteria by measuring the contact angle [42]. For this reason, the contact angle of the thin films and the substrate (314SS) was analysed using the sessile drop technique (Figure 5).

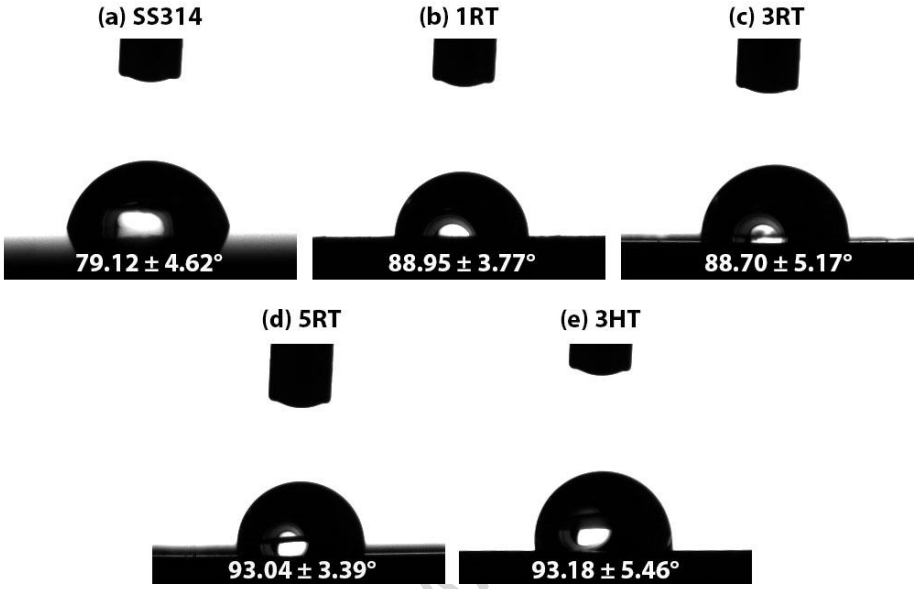

Figure 5 Average water contact angle for SS314 and the analysed Cu-Zr thin films

The contact angle measured for the stainless steel substrate was 79.12 ± 4.62°, which is smaller than for the Cu-Zr thin films: 88.95 ± 3.77° (1RT), 88.70 ± 5.17° (3RT), 93.04 ± 3.39° (5RT) and 93.18 ± 5.46° (3HT). The contact angle for SS314 is therefore the smallest, while a slight increase in contact angle can be noticed as the chamber pressure and temperature rises. These values of contact angle for Cu-Zr thin films of around 90 degrees, are comparable to the values obtained by Zeman et al. [43] for Cu-Zr thin films in the compositional range 10-90 Cu at. % (87° to 108°). On the other hand, they are slightly higher than that reported for other Cu-based thin films like $Cu_{90}Ti_{10}$ (74.1°) [12] but lower than for Cu-rich alloys such as $Zr_{53}Cu_{30}Ni_9Al_8$ (between 99.5° and 104.0°) [44]. The wettability depends on numerous parameters such as the surface roughness, as observed by Kubiak et al. [45]. In this paper, the authors showed that the apparent contact angle decreases with increasing roughness up to about 300 µm. The measurements obtained seem to follow this trend, however, there are some discrepancies since for 3HT the contact angle is maximum (93.18 ± 5.46°) but the roughness is not minimum (i.e., it is higher than for 3RT and 5RT). In any case, differences in contact angle are practically within the error range.

3.3. Influence of drying on the recovery of bacteria from surfaces

In order to assess the influence of drying on the recovery of bacteria from metallic surfaces, *E. coli* and *S. aureus* were applied to stainless steel 314 (a corrosion resistant material without antimicrobial activity that can be used as a control) and subsequently recovered, plated and counted. Figure 6 shows the number of colony forming units (CFU) per millilitre recovered in dry conditions for 0, 15, 30 and 45 min contact times. The recovery of bacteria diminished with increasing contact times from ~10^8 (0 min) to ~10^4 (45 min) for *E. coli* and from ~10^9 (0 min) to ~10^8 (45 min) for *S. aureus*, therefore the largest reduction (i.e., 5 $\log_{10}$) was detected for *E. coli*. The difference in recovery rates between *E. coli* and *S. aureus* are interesting and not easily explained by reference to a single factor. In general, Gram positive bacteria (like *S. aureus*) tolerate desiccation better than Gram-negative bacteria (like *E. coli*) [46] but it is important that the lack of recovery here is not interpreted as death, especially over the short times applied in this study. The lack of recovery may also reflect a more avid binding of the bacteria promoted by the desiccation of its outer layers or by adaptive responses to their new environment, for instance the synthesis of adhesion molecules.

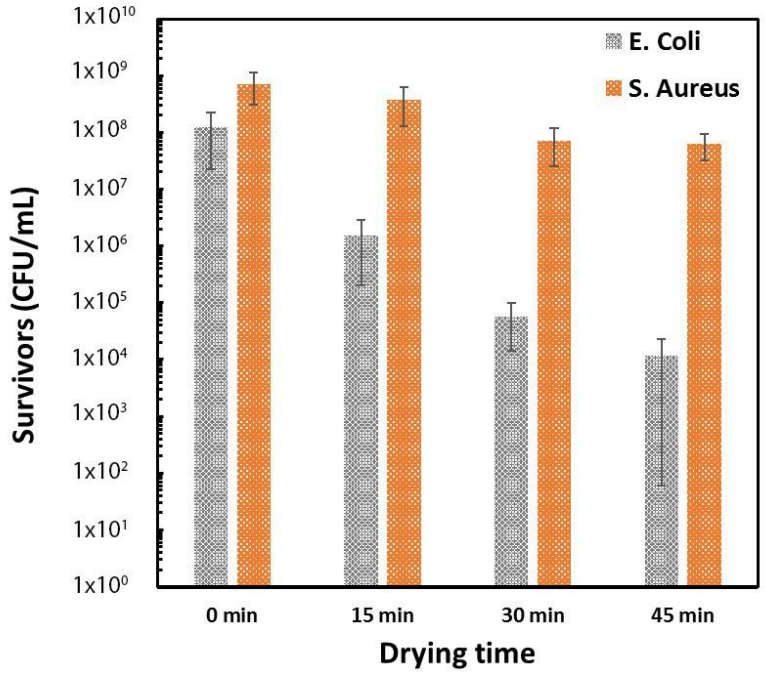

Figure 6 Recovery of *E. coli* and *S. aureus* deposited on 314SS for "dry" conditions after 0, 15, 30 and 45 min contact time. Each surface was inoculated with 2 µL of bacteria culture growth until OD_{600}~0.3.

To investigate the drying effect in more detail, the morphological differences of *E. coli* and *S. aureus* have been studied in “wet” and “dry” conditions using SEM. *E. coli* cells fixed in “wet” conditions (Figure 7a) consist of relatively smooth surfaces, revealing the presence of low bumps and valleys from the outer membrane layer. On the other hand, the *E. coli* cells in “dry” conditions (Figure 7c) exhibit slight morphological differences. The width of the “dry” cells is slightly smaller (0.7 μm in the healthy bacteria to 0.5 μm in the “dry” cells) while the length of wet and dry *E. coli* bacteria is about 2.5 μm. In addition, the surface morphology is slightly different, with the “dry” cells displaying a shrivelled outer membrane.

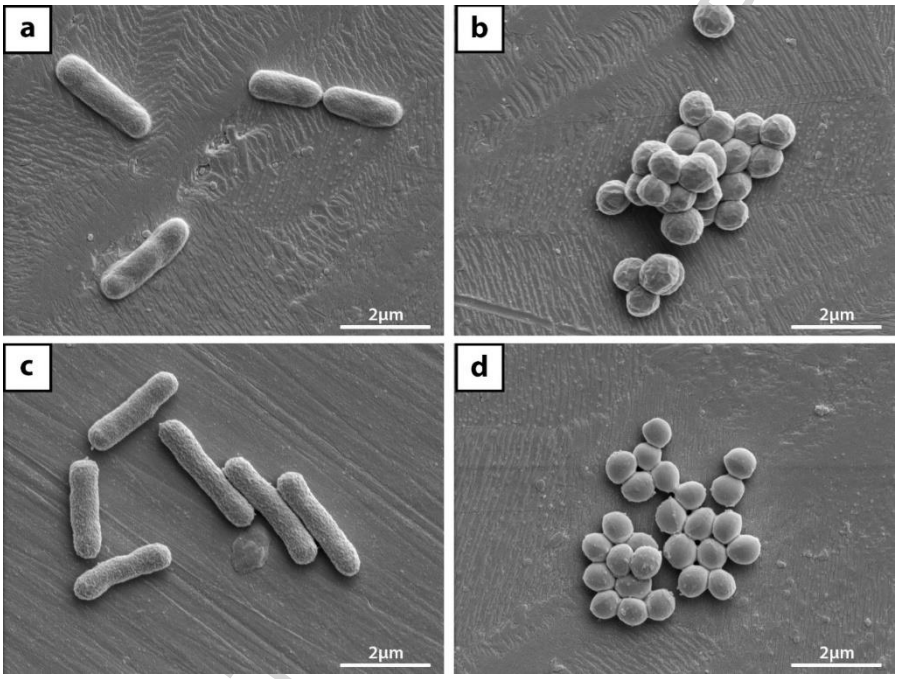

Figure 7 Secondary electron images for “wet” conditions, *E.coli* and *S. aureus* (a,b) and “dry” conditions for *E. coli* and *S. aureus* (c,d) deposited on 314SS after 1h.

The *S. aureus*, undried samples (Figure 7b) display a rough surface; while the dried samples seem smoother (Figure 7d). The morphological differences might be attributed to the removal of the outer “fuzzy” layer of fine fibres of teichoic acids and proteins during the cell processing (i.e., SEM fixing) and upon drying [47]. The drying of the cells could have damaged the agglomeration of fine fibres attached to the peptidoglycan layer, which could be removed during the fixing. Then, the smooth surface observed in Figure 7d will be the thick peptidoglycan layer common to Gram Positive bacteria [47].

The reduction in colony forming units in “dry” conditions for the 314 SS substrate cannot be attributed to the materials since it lacks any antimicrobial behaviour. Therefore, it should be

mostly attributed to the drying of the LB broth. To investigate this in more detail, 314SS samples were inoculated with pure broth and subsequently observed in the SEM. Once the broth dries, a substance of dendritic geometry was observed on the surface of the samples. EDX measurements indicated a composition of $C_{60.0}Cl_{14.2}Na_{13.9}O_{8.6}Zn_{0.5}Cu_{0.4}K_{0.2}P_{0.2}Fe_{0.2}S_{0.1}$ at. %. Consequently, the dendrites are expected to be crystals of sodium chloride and other components of the LB broth used in the tests (Luria Bertani broth: Peptone 10 g/L, Yeast 5 g/L and NaCl 5 g). The increasing sodium chloride concentration experienced by the bacteria during the evaporation of the water may have some impact on their differential recovery (Figure 6) as *S. aureus* is particularly halotolerant [48], but it should be noted that this is a short-lived temporary state in the transition to dryness. Consequently, the composition of LB broth has to be carefully selected to develop "dry" antimicrobial tests.

3.4. "Wet" vs "Dry" antimicrobial tests

The antimicrobial properties of all thin films was assessed by the differential reduction in recovery of *E. coli* and *S. aureus* recovered from the coated and uncoated surfaces over time in "wet" and "dry" conditions. The influence of drying on recovery of *E. coli K12* described above would greatly complicate the analysis and, consequently, only *S. aureus* cells were used to compare the "wet" and "dry" methodologies. This focus on *S. aureus* is warranted as, unlike *E. coli*, it is often found on human skin and is relevant for surface transmission in healthcare and other settings [49].

Figure 8 shows the number of *S. aureus* recovered in "wet" and "dry" assay conditions for 1, 2.5 and 4 hours contact time. The stainless steel coupons (314SS) show a relatively consistent recovery of bacteria for both "wet" (~$3x10^8$ CFU/mL) and "dry" (~$5x10^7$ CFU/mL) conditions, especially for the "wet" tests. For the "dry" applications, the number of cells has not only been reduced when compared to the "wet" conditions (from ~$3x10^8$ CFU/mL to ~$8x10^7$ CFU/mL), but less cells were recovered during the next 1.5 hours (to about ~$5x10^7$ CFU/mL). As steel does not have any antimicrobial activity this reduction must have been caused during the drying process and was taken into account to obtain a reliable antimicrobial activity result.

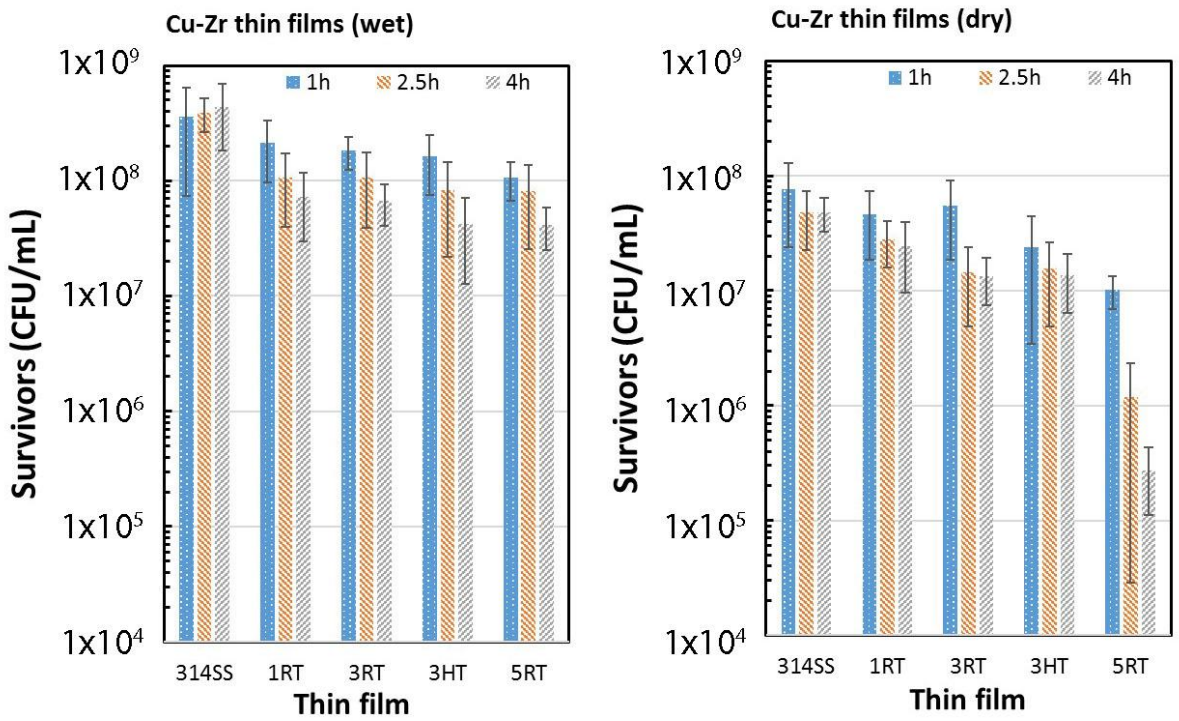

Figure 8 Recovery of *S. aureus* (Colony Forming Units per mL) after 1h, 2.5 h and 4 h for the Cu-Zr thin films analysed in wet and dry conditions.

For the "wet" thin films, the bacteria recovery is similar during the first hour of contact killing (~$2x10^8$ CFU/mL) with a slight decrease in recovered bacteria as the contact time increases. This decrease is similar in the 1RT and 3RT films, while the 3HT and 5RT samples reveal a slight decrease (to about ~$3x10^7$ CFU/mL). For the "dry" tests, the number of recovered bacteria are lower than those of the "wet" conditions, but the antimicrobial behaviour follows a similar trend. The sample deposited with the lower chamber pressure (1RT) continues to display the highest number of recovered bacteria (with a minimum of ~$2x10^7$ CFU/mL), indicating low antimicrobial properties. In contrast, the 3RT thin film has been able to lower the number of recovered bacteria to levels similar to those of 3HT (~$1x10^7$ CFU/mL after 4 h of contact killing). However, the thin films with lowest number of surviving bacteria are those deposited at 0.5 Pa (5RT), reaching minimums of about $2x10^5$ CFU/mL, which is two orders of magnitude lower than that for the thin films grown at lower pressures of 0.1 Pa (1RT) and 0.3 Pa (3RT).

The antimicrobial activity and percentage of reduction were calculated using the equations provided by the Japanese JIS Z2801:2010 "Antibacterial products—Test for antibacterial activity and efficacy" (Table 4) and the American US EPA "Protocol for the Evaluation of

Bactericidal Activity of Hard, Non-Porous Copper Containing Surface Products" (Table 5) respectively. The resulting antimicrobial activity and percentage reduction were calculated using the number of viable colony forming units of stainless steel in "wet" or "dry" conditions as a reference, since this material does not possess any antimicrobial behaviour (i.e. antimicrobial activity and reduction percentage values of 0 and 0.00% respectively, for more details see [22]). Both results have been shown for comparison purposes since the Japanese standard gives an accurate estimation of the antimicrobial performance due to the logarithmic scale (log_{10} reduction), while the American standard provides a more intuitive result (percentage reduction). It should be noted that we use significantly higher bacterial challenges (i.e. ~$3x10^8$ CFU/mL) than those defined in these standards (i.e. $2.5x10^5$ to $1x10^6$ CFU/mL) in order to be able to perceive activity differences with greater resolution.

Table 4 Antimicrobial activity calculated as stated in JIS Z 2801:2010 "Antibacterial products—test for antibacterial activity and efficacy" for the Cu-Zr thin films after 1, 2.5 and 4h of contact killing.

	Antimicrobial activity					
Sample	Wet			Dry		
	1h	2.5h	4h	1h	2.5h	4h
1RT	0.23	0.56	0.77	0.22	0.23	0.29
3RT	0.30	0.56	0.81	0.15	0.53	0.55
5RT	0.53	0.68	1.02	0.88	1.61	2.25
3HT	0.35	0.67	1.01	0.51	0.49	0.54

Table 5 Percentage reduction calculated as stated in U.S. EPA "Protocol for the Evaluation of Bactericidal Activity of Hard, Non-Porous Copper-Containing Surface Products" for the Cu-Zr thin films after 1, 2.5 and 4h of contact killing.

	Percentage reduction					
Sample	Wet			Dry		
	1h	2.5h	4h	1h	2.5h	4h
1RT	28.14	56.87	74.66	12.02	64.09	51.09
3RT	33.78	60.02	80.40	18.41	83.07	73.91
5RT	61.55	67.82	83.90	94.50	99.20	99.47
3HT	45.63	65.90	83.15	70.00	75.98	74.16

The data described here have been adjusted for loss of recovery due to drying and can be considered as losses due to cell death. In general for the "wet" tests recovery of viable bacteria decreases as the contact time increases, however, the antimicrobial activity is low, between 0.77 and 1.02 log_{10} reductions and percentage reductions between 74.66 % and

83.90 %. The increase in deposition pressure, as well as the increase in substrate temperature reveals superior antimicrobial activity. The activity in “wet” conditions for the 5RT sample is similar to that observed for the 3HT film, suggesting that, besides chemical composition, the film deposition parameters can influence the antibacterial properties of the material. This idea was previously proposed by Chiang et al. [1] who revealed that variations in target power during deposition had an influence on the antimicrobial properties of *E. coli* cells deposited on $Zr_{61}Al_{7.5}Ni_{10}Cu_{17.5}Si_4$ thin films. It should be noted that higher antimicrobial reductions of thin films can be found in the literature, but most of them involve much longer contact times (i.e., 24h), limiting their possible application as antimicrobial touch surfaces [3, 50]. These low antimicrobial properties are consistent with the nanograin structure of the deposited thin films which limits the diffusion of copper ions [17].

The same trend can be observed for the “dry” tests. Overall, four hours of contact killing eliminated a small number of cells, between 0.29 to 0.55 $\log_{10}$ values of antibacterial activity, or reduction of bacteria percentage between 51.09 % and 74.16 %, for the Cu-Zr films deposited at the lower pressures (1RT and 3RT) as well as that with substrate heating (3HT). The lower concentration of *S. aureus* cells caused by the drying of the surface, has not increased the antimicrobial rates, contradicting the idea that drying may increase the copper intake of bacteria [23, 24]. Interestingly, the film deposited at room temperature and 0.5 Pa (5RT) exhibited better antimicrobial rates (2.25 $\log_{10}$ reduction or 99.47 %) after just 4 h, which is similar to that reported for other thin films after 24 h of contact time [3]. The increase in antimicrobial performance can be explained by the compactness of the films seen in Figure 1. The most compact thin film (1RT) will be unable to release high amounts of Cu ions, limiting bacterial exposure. As the pressure and deposition temperature increased (3RT and 3HT), film compactness decreased and the antimicrobial activity improved, reaching a maximum in samples deposited at 0.5 Pa (5RT). This result can be related to Thornton’s structural zone model [34] (see Figure 2), where increasing substrate temperature and lower sputtering pressure leads to a more compact and dense film.

To better understand the reason for the antimicrobial behaviour under the different processing conditions, the surface morphology of *S. aureus* have been studied under the SEM for the two most extreme conditions, 1RT and 5RT in “dry” and “wet” conditions (Figure 9). For the 1RT sample, the contact in “wet” conditions (Figure 9a) reveals the expected spherical shape proper of cocci, while the antimicrobial tests in “dry” conditions (Figure 9c) seem to have cells with a smoother surface. This change between “wet” (Figure 9b) and “dry” (Figure 9d) is more pronounced in cells deposited on the 5RT thin film. The contact

between *S. aureus* cells and copper has been reported to cause damage to the cell in the form of flattening, pitting and lysis [51, 52]. However, the lack of these defects seems to indicate that such low contact times (1-4 h) did not result in a marked loss of integrity for *S. aureus*, suggesting that the antimicrobial mechanisms responsible for the killing of bacteria generate more subtle damage to essential proteins and DNA that has removed the ability of the cells to replicate.

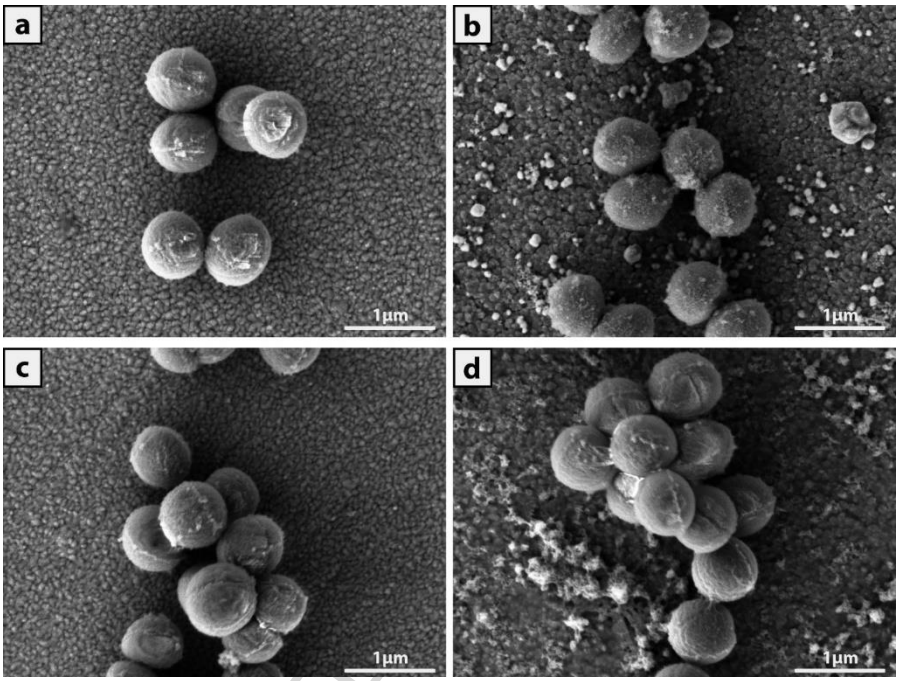

Figure 9 Secondary electron SEM images showing the morphology of *S. aureus* in 1RT a) "wet" and c) "dry" conditions and 5RT in b) "wet" and d) "dry" conditions after 4h of contact killing.

To understand the mechanisms of copper diffusion and estimate the corrosion of the deposited thin films, SEM images of the samples were taken after 4 h of contact killing (Figure 10). The surface of the samples 1RT, 3RT and 3HT prepared in "wet" conditions do not display great changes, while the surface of the 5RT thin film has developed a rougher surface with protrusions growing from its surface. On the other hand, after "dry" applications of bacteria on both 3HT and 5RT samples, surface cracks are evident, especially for the 5RT sample, where some pits could be observed. In contrast, the 3RT sample showed minor changes, while the surface of the 1RT sample remained unchanged.

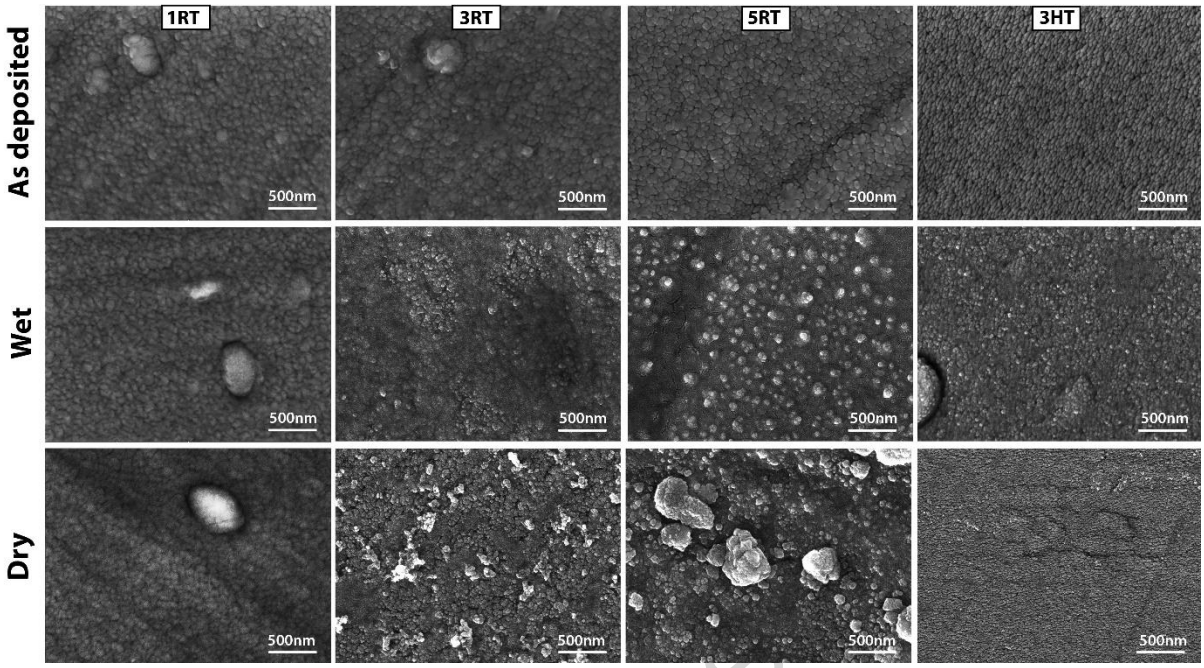

Figure 10 Secondary electron SEM images of the thin films surface in the as deposited conditions and after the antimicrobial tests in “dry” and “wet” conditions after 4h of contact killing.

No great surface changes were observed for the 1RT and 3RT samples, while little degradation (i.e. pitting) of the films could be noticed in the 3HT and 5RT films for the dry conditions (not shown in the images). The results of Bouala et al. [3] and Etiemble et al. [53] suggest that chloride-containing media, such as the culture broth used for this research, can increase the flow of Cu ions into the deposited bacteria. This process can only take place when the anodic potential is higher than the equilibrium potential of Cu/Cu^{+2} [54]. The addition of Cl^- ions in concentrations higher than 0.01 mol/L can promote the formation of CuCl thus increasing the transfer of metallic ions to the contact media [54]. In our experiments, the LB broth contains 5 g/L of NaCl (0.141 mol/L of Cl^-), much higher than 0.01mol/L, and therefore it favours the release of Cu ions. Pitting and cracking similar to the ones shown in Figure 10 can be found in the literature as a sign of corrosion due to the presence of chlorine salts in Cu-based thin films [3, 53]. Considering the available literature, and our own antimicrobial results, it seems likely that the changes in antimicrobial properties between “dry” and “wet” conditions have been caused by a higher degradation of the film, induced by the increase in NaCl during the evaporation of the LB broth. This will explain the higher antimicrobial properties of the 5RT film, as the surface degradation will be higher due to the lower density and compactness of the film shown by Thornton’s model [34] (Figure 2).

To analyse the copper ion release, ICP-OES measurements of thin films produced under the two most extreme conditions (1RT and 5RT) were taken in both “dry” and “wet” conditions (Table 6). Although the error bars of these measurements are high, some interesting differences can be observed. The ion release test reveal higher copper values for the films deposited at 0.5 Pa, with a maximum of 1088.13 ± 305.19 ppb after 4 h in “wet” conditions. This agrees with the more porous structure revealed from the cross section analysis (Figure 1), thus suggesting that the changes in compactness shown by Thornton’s SZM are a good indicator of changes in the copper ion diffusion. For both thin films, the release of copper ions rises as the contact time increases from 1 to 4 h, which concurs with the reduction in viable bacteria. It is of interest to notice that for 1RT, the thin film with highest compactness, the number of copper ions in “wet” conditions is lower than those measured in “dry” conditions (i.e. 132.60 ± 49.89 ppb in the former and 262.21 ± 81.34 ppb in the latter). However, after 4 h of contact this trend reverses, with higher copper ion release in the “wet” conditions (i.e. 349.51 ± 139.37 ppb in the former and 270.45 ± 74.40 ppb in the latter). This phenomena is not observed in the less compact film (5RT), where the number of copper ions diffused is always higher in the “wet” conditions, which may be a result of surface damage promoted by the formation of sodium chloride crystals. The copper ion release from the Cu-Zr thin films is much higher than those reported by Chu et al. [44] (i.e. 45 ppb after 24 h of contact). However, the copper content of our samples is 85 at. %, while for the Zr-Cu-Ni-Al alloy deposited in the aforementioned paper the maximum copper content is 30 at. %.

Table 6 Copper ion release (ppb) for the 1RT and 5RT thin films

	Contact time			
	1h		4h	
Condition	wet	dry	wet	dry
1RT	132.60 ± 49.89	262.21 ± 81.34	349.51 ± 139.37	270.45 ± 74.40
5RT	841.43 ± 267.77	632.24 ± 192.22	1088.13 ± 305.19	934.97 ± 103.77

3.5. TEM analysis

To understand the morphological changes driven by copper to *E. coli* and *S. aureus*, TEM images (Figure 11) were taken from bacteria recovered from the 314SS and the thin film with highest antimicrobial activity (5RT) after 4h of “dry” contact. *E. coli* cells recovered from steel (Figure 11a) reveal an undamaged cell membrane similar to those reported in other TEM analyses [55]. On the other hand, exposure to the Cu-based thin films (Figure 11c) has led to a partial lysis (i.e. disintegration of a cell by rupture of the cell wall or membrane). In

addition, dark spots can be observed in the cytoplasm of the cell that may be attributed to copper oxidation during the denaturation of proteins [56, 57]. Damage to the exterior of *E. coli* in the form of cell shrinkage, apparition of pits and cavities and loss of its natural rod shape is commonly reported in the literature as a direct effect of copper contact with *E. coli* [56, 58, 59]. The TEM images reveal that while some degree of damage has been done to the cell membrane, it has not been enough to affect its rod-like morphology. The irregular outer layer observed in Figure 7c would have increased the inflow of copper ions into the cell, confirming the idea that copper ions alter the permeability of cellular membranes and destabilize the cell wall [56, 59]. At the same time, the high affinity of Cu^{2+} ions with phosphorus- and sulphur- containing compounds rich in the inner part of the cells will further the damage, conferring copper its high contact killing properties [44, 60].

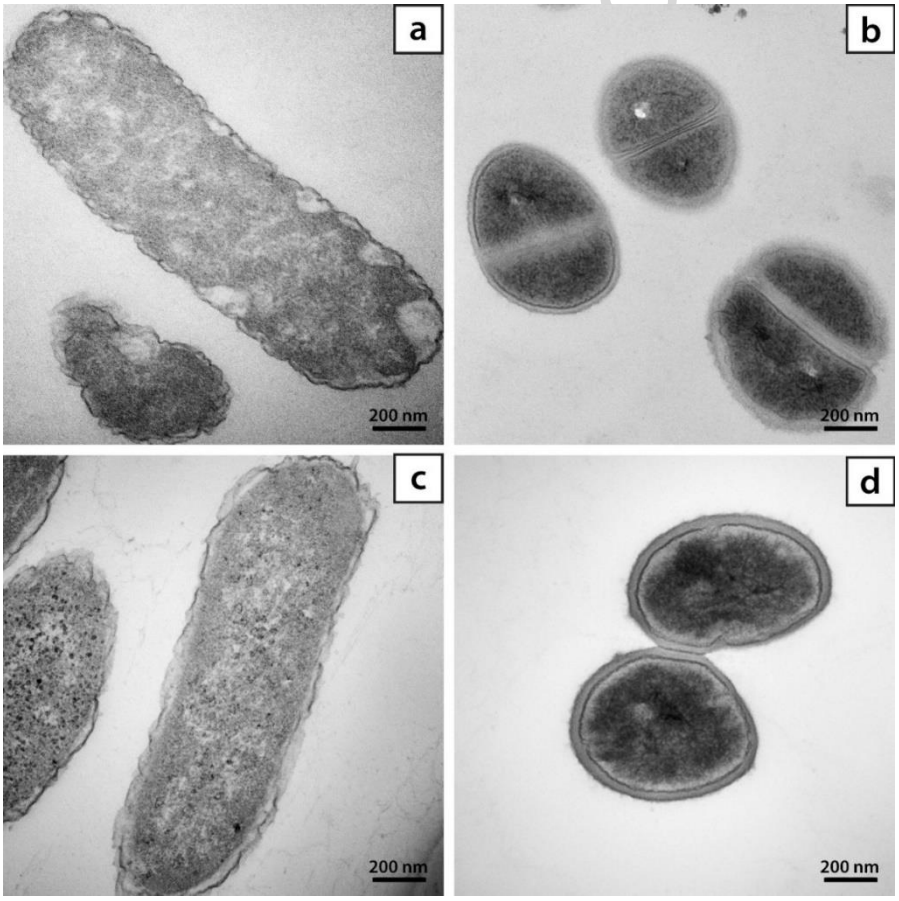

Figure 11 TEM images of *E. coli* and *S. aureus* cells deposited on steel (a, b) and Cu-Zr thin film for 5RT condition (c, d) after 4h of “dry” contact.

For the *S. aureus* deposited on steel (Figure 11b) and Cu-Zr thin film (Figure11d), the cells retain the morphology typical of coccus. The cell wall reveals a slight detachment from the cytoplasmic membrane with punctual lysis and a clear decolouration surrounding the inner

side of this membrane. These results are in agreement with the limited outer damaged observed in the SEM imaging of both GP and GN bacteria (Figures 9b and 9d), supporting the idea of inner damage. Analysis of cell damage in other Gram positive cocci (i.e. *Streptococcus mutans*) deposited on copper-rich surfaces indicates progressive damage to the cell wall [61], but the timeframes are much longer (up to 24 h) than those used in the present work (up to 4 h). In addition, *S. aureus* is more resistant to damage caused by copper due to their the ability to agglomerate and the numerous mechanisms available to resist environmental copper [62]. Consequently, it is reasonable to anticipate that obvious cell damage will not be discerned for short timeframes.

4. Conclusions

In this work we have shown that the Thorton's structural zone model provides sensitive enough information to observe differences in the microstructures of Cu-Zr thin films grown at varying sputtering pressure and substrate temperature, even within the same structure zone of the model. While other authors have focused on structural variations at different zones of the model (i.e., at very different processing conditions), we have proven that, at least for the Cu-Zr system, even within the same zone it is possible to detect differences in antimicrobial behaviour.

The evolution of the antimicrobial behaviour over the contact time is, in general, not higher in "dry" than in "wet" conditions and therefore the copper ion diffusion over the contact time is similar. However, for the least compact Cu-Zr thin film grown at 0.5 Pa (5RT) the evolution of the antimicrobial behaviour over the contact time is much higher in "dry" than in "wet" conditions and is significantly higher than that for films grown at lower pressures of 0.1 Pa (1RT) and at 0.3 Pa, both with and without substrate heating (3HT and 3RT). These results suggest that for "dry" tests to provide higher antimicrobial performance than "wet" tests, the thin film structure should exhibit low compactness. This suggestion is further supported by the higher copper ions measured in these samples.

TEM analysis of *E. coli* and *S. aureus* after 4 h of "dry" contact with Cu-Zr thin films show that both exhibit partial lysis and inner damage but not enough to result in morphological changes of the bacteria.

5. Acknowledgments

The authors acknowledge research support from Northumbria University. We acknowledge G. Wells and the Smart materials and Surfaces Laboratory from Northumbria University for the support with the sessile drop test, Kathryn White and

Tracey Davey from Newcastle Medical School are acknowledged for the support with TEM sample preparation and Rob Dixon from Newcastle University for the support with ICP-OES

6. References

[1] P.T. Chiang, G.J. Chen, S.R. Jian, Y.H. Shih, J.S.C. Jang, C.H. Lai, Surface antimicrobial effects of Zr61Al7.5Ni10Cu17.5Si4 thin film metallic glasses on Escherichia coli, Staphylococcus aureus, Pseudomonas aeruginosa, Acinetobacter baumannii and Candida albicans. Fooyin J. Health Sci. 2 (2010) 12-20.
[2] Y.Y. Chu, Y.S. Lin, C.M. Chang, J.K. Liu, C.H. Chen, J.C. Huang, Promising antimicrobial capability of thin film metallic glasses. Mater. Sci. Eng. C (2014) 221-225.
[3] G.N. Bouala, A. Etiemble, C.d. Loughian, C. Langlois, J.F. Pierson, P. Steyer, Silver influence on the antibacterial activity of multi-functional Zr-Cu based thin film metallic glasses. Surf. Coat. Technol. (2017).
[4] J.A. Lemire, J.J. Harrison, R.J. Turner, Antimicrobial activity of metals: mechanisms, molecular targets and applications. Nat. Rev. Microbiol 11 (2013) 371–384.
[5] H.T. Michels, J.O. Noyce, C.W. Keevil, Effect of temperature and humidity on the efficacy of methicillin-resistant Staphylococus aureus challenged antimicrobial materials containing silver and copper. Lett. Appl. Microbiol. 49 (2009) 191-195.
[6] D.J. Barillo, D.E. Marx, Silver in medicine: A brief history BC 335 to present. Burns 40 (2014) S3-S8.
[7] J.L. Clement, P.S. Jarrett, Antibacterial Silver. Met. Based Drugs 1 (1994) 467-462.
[8] M. Rai, A. Yadav, A. Gade, Silver nanoparticles as a new generation of antimicrobials. Biotechnol. Adv. 27 (2009) 76-83.
[9] E. Zhang, L. Zheng, J. Liu, B. Bai, C. Liu, Influence of Cu content on the cell biocompatibility of Ti–Cu sintered alloys. Mater. Sci. Eng. C 46 (2015) 148-157.
[10] O.I. Aruoma, B. Halliwell, E. Gajewski, M. Dizdaroglu, Copper-ion dependent damage to the bases in DNA in the presence of hydrogen-peroxide. J. Biol. 273 (1991) 601–604.
[11] L. Banci, I. Bertini, F. Cantini, S. Ciofi-Baffoni, Cellular copper distribution: a mechanistic systems biology approach. Cell. Mol. Life Sci. 67 (2010) 2563–2589.
[12] D. Wojcieszak, D. Kaczmarek, A. Antosiak, M. Mazur, Z. Rybak, A. Rusak, M. Osekowska, A. Poniedzialek, A. Gamian, B. Szponar, Influence of Cu–Ti thin film surface properties on antimicrobial activity and viability of living cells. Mater. Sci. Eng. C 56 (2015) 48-56.
[13] M.F. Ashby, A.L. Greer, Metallic glasses as structural materials. Scr. Mater. 54 (2006) 321-326.
[14] T. Gloriant, Microhardness and abrasive wear resistance of metallic glasses and nanostructured composite materials. J. Non. Cryst. Solids 316 (2003) 96-103.
[15] B. Lin, R. Mu, L. Yang, X. Bian, Antibacterial effect of metallic glasses. Chin. Sci. Bull. 57 (2012) 1069-1072.
[16] L. Huang, E.M. Fozo, T. Zhang, P.K. Liaw, W. He, Antimicrobial behaviour of Cu-bearing Zr-based bulk metallic glasses. Mater. Sci. Eng. C 39 (2014) 325-329.
[17] V.M. Villapún, H. Zhang, C. Howden, L.C. Chow, F. Esat, P. Pérez, J. Sort, S. Bull, J. Stach, S. González, Antimicrobial and wear performance of Cu-Zr-Al metallic glass composites. Materials & Design 115 (2017) 93-102.
[18] A. Shibata, Y. Imamura, M. Sone, C. Ishiyama, Y. Higo, Pd-Ni-P metallic glass film fabricated by electroless alloy plating. Thin Solid Films 517 (2009) 1935-1938.
[19] Q. Guo, J.H. Noh, P.K. Liaw, P.D. Rack, Y. Li, C.V. Thompson, Density change upon crystallization of amorphous Zr-Cu-Al thin films. Acta Mater. 58 (2010) 3633-3641.

[20] Y.P. Deng, Y.F. Guan, J.D. Fowlkes, S.Q. Wen, F.X. Liu, G.M. Pharr, P.K. Liaw, C.T. Liu, P.D. Rack, A combinatorial thin film sputtering approach for synthesizing and characterizing ternary ZrCuAl metallic glasses. Intermetallics 15 (2007) 1208-1216.
[21] L. Xie, P. Brault, A.-L. Thomann, L. Bedra, Molecular dynamic simulation of binary ZrxCu100-x metallic glass thin film growth. Appl. Surf. Sci. 274 (2013) 164-170.
[22] V.M. Villapún, L.G. Dover, A. Cross, S. González, Antibacterial metallic touch surfaces. Materials 9 (2016) 736.
[23] S.L. Warnes, C.W. Keevil, Inactivation of norovirus on dry copper alloy surfaces. PloS one 8 (2013) e75017.
[24] C.E. Santo, E.W. Lam, C.G. Elowsky, D. Quaranta, D.W. Domaille, C.J. Chang, G. Grass, Bacterial killing by dry metallic copper surfaces. Appl. Environ. Microbiol. 77 (2011) 794-802.
[25] J.K.M. Knobloch, S. Tofern, W. Kunz, S. Schütze, M. Riecke, W. Solbach, T. Wuske, "Life-like" assessment of antimicrobial surfaces by a new touch transfer assay displays strong superiority of a copper alloy compared to silver containing surfaces. PloS one 12 (2017) e0187442.
[26] P. Louis, H.G. Trüper, E.A. Galinski, Survival of Escherichia coli during drying and storage in the presence of compatible solutes. Appl. Microbiol. Biotechnol. 28 (1994) 390-402.
[27] A.C. Baird-Parker, E. Davenport, The effect of recovery medium on the isolation of Staphylococcus aureus after heat treatment and after the storage of frozen or dried cells. J. Appl. Microbiol. 28 (1965) 390-402.
[28] V.M. Villapún, F. Esat, S. Bull, L.G. Dover, S. Gonzalez, Tuning the Mechanical and Antimicrobial Performance of a Cu-Based Metallic Glass Composite through Cooling Rate Control and Annealing. Materials 10 (2017) 506.
[29] E.R. Fischer, B.T. Hansen, V. Nair, F.H. Hoyt, D.W. Dorward, Scanning Electron Microscopy. Curr. Protoc. Microbiol. 25:B:2B.2:2B.2.1–2B.2.47. (2012).
[30] D. Depla, On the effective sputter yield during magnetron sputter deposition. Nucl. Instrum. Methods Phys. Res. B 328 (2014) 65-69.
[31] C.V. Thompson, R. Carel, Stress and grain growth in thin films. J. Mech. Phys. Solids. 44 (1996) 657-673.
[32] C.V. Thompson, Grain growth in polycrystalline thin films of semiconductors. Interface Sci. 6 (1998) 85-93.
[33] K. Chan, T. Tou, B. Teo, Effect of substrate temperature on electrical and structural properties of copper thin films. Microelectronics J. 37 (2006) 930-937.
[34] J.A. Thornton, High rate thick film growth. Annual review of materials science. Annu. Rev. Mater. Sci. 7 (1977) 239-260.
[35] H. Okamoto, Cu-Zr (copper-zirconium). Journal of phase equilibria and diffusion 29 (2008) 204-204.
[36] J.A. Thornton, Recent Developments in Sputtering--Magnetron Sputtering. Metal Finishing 77 (1979) 83-87.
[37] P.J. Kelly, R.D. Arnell, Magnetron sputtering: a review of recent developments and applications. Vacuum 56 (2000) 159-172.
[38] J. Musil, Flexible hard nanocomposite coatings. RSC Adv. 5 (2015) 60482-60495.
[39] Y.J. Park, Y.H. Song, J.H. An, H.J. Song, K.J. Anusavice, Cytocompatibility of pure metals and experimental binary titanium alloys for implant materials. J. Dent. 41 (2013) 1251–1258.
[40] A. Shedle, P. Samorapoompichit, X.H. Rausch-Fan, A. Franz, W. Fureder, W.R. Sperr, W. Sperr, A. Ellinger, R. Slavicek, G. Boltz-Nitulescu, P. Valent, Response of L-929 fibroblasts, human gingival fibroblasts, and human tissue mast cells to various metal cations. J. Dent. Res. 74 (1995) 1513–1420.
[41] A. Yamamoto, R. Honma, M. Sumita, Cytotoxicity evaluation of 43 metal salts using murine fibroblasts and osteoblastic cells. J. Biomed. Mater. Res. 39 (1998) 331–340.
[42] L.K. Ista, S. Mendez, G.P. Lopez, Attachment and detachment of bacteria on surfaces with tunable and switchable wettability. Biofouling 26 (2010) 111-118.

[43] P. Zeman, M. Zitek, S. Zuzjaková, R. Čerstvý, Amorphous Zr-Cu thin-film alloys with metallic glass behavior. J. Alloys Compd. 696 (2017) 1298-1306.
[44] J.H. Chu, J. Lee, C.C. Chang, Y.C. Chan, M.L. Liou, J.W. Lee, J.S.C. Jang, J.G. Duh, Antimicrobial characteristics in Cu-containing Zr-based thin film metallic glass. Surf. Coat. Technol. 259 (2014) 87-93.
[45] K.J. Kubiak, M.C.T. Wilson, T.G. Mathia, P. Carval, Wettability versus roughness of engineering surfaces. Wear 271 (2011) 523-528.
[46] M. Potts, S.M. Slaughter, F.U. Hunneke, J.F. Garst, R.F. Helm, Desiccation tolerance of prokaryotes: application of principles to human cells. Integr. Comp. Biol. 45 (2005) 800-809.
[47] A. Umeda, Y. Ueki, K. Amako, Structure of the Staphylococcus aureus cell wall determined by the freeze-substitution method. J. Bacteriol. 169 (1987) 2482-2487.
[48] M. Hajmeer, E. Ceylan, J.L. Marsden, D.Y. Fung, Impact of sodium chloride on Escherichia coli O157: H7 and Staphylococcus aureus analysed using transmission electron microscopy. Food Microbiol. 23 (2006) 446-452.
[49] R.W. Bauman, E. Machunis-Masuoka, I.R. Tizard, Microbiology: with diseases by taxonomy, Benjamin Cummings, California, 2011.
[50] J. Lee, M.L. Liou, J.G. Duh, The development of a Zr-Cu-Al-Ag-N thin film metallic glass coating in pursuit of improved mechanical, corrosion, and antimicrobial property for bio-medical application. Surf. Coat. Technol. 310 (2017) 214-222.
[51] D. Sun, D. Xu, C. Yang, M.B. Shahzad, Z. Sun, J. Xia, J. Zhao, T. Gu, K. Yang, G. Wang, An investigation of the antibacterial ability and cytotoxicity of a novel cu-bearing 317L stainless steel. Sci. Rep. 6 (2016) 29244.
[52] B. Subramanian, S. Maruthamuthu, S.T. Rajan, Biocompatibility evaluation of sputtered zirconium-based thin film metallic glass-coated steels. Int. J. Nanomedicine 10 (2015) 17.
[53] A. Etiemble, C.d. Loughian, M. Apreutesei, C. Langlois, S. Cardinal, J.M. Pelletier, J.F. Pierson, P. Steyer, Innovative Zr-Cu-Ag thin film metallic glass deposed by magnetron PVD sputtering for antibacterial applications. J. Alloys Compd. 707 (2017) 155-161.
[54] H.B. Lu, L.C. Zhang, A. Gebert, L. Schultz, Pitting corrosion of Cu–Zr metallic glasses in hydrochloric acid solutions. J. Alloys Compd. 462 (2008) 60-67.
[55] M.E. Hayat, Fixation for electron microscopy, Academic Press, London, 1981.
[56] M. Raffi, S. Mehrwan, T.M. Bhatti, J.I. Akhter, A. Hameed, W. Yawar, M.M.u. Hasan, Investigations into the antibacterial behavior of copper nanoparticles against Escherichia coli. Ann. Microbiol. 60 (2010) 75-80.
[57] M. Khalaj, M. Kamali, Z. Khodaparast, A. Jahanshahi, Copper-based nanomaterials for environmental decontamination–An overview on technical and toxicological aspects. Ecotoxicol. Environ. Saf. 148 (2018) 813-824.
[58] Y. Liu, J. Padmanabhan, B. Cheung, J. Liu, Z. Chen, B.E. Scanley, D. Wesolowski, M. Pressley, C.C. Broadbridge, S. Altman, U.D. Schwarz, T.R. Kyriakides, J.Schroers, Combinatorial development of antibacterial Zr-Cu-Al-Ag thin film metallic glasses. Sci. Rep. 6 (2016) 26950.
[59] U. Bogdanović, V. Lazić, V. Vodnik, M. Budimir, Z. Marković, S. Dimitrijević, Copper nanoparticles with high antimicrobial activity. Mater. Lett. 128 (2014) 75-78.
[60] A.K. Chatterjee, R.K. Sarkar, A.P. Chattopadhyay, P. Aich, R. Chakraborty, T. Basu, A simple robust method for synthesis of metallic copper nanoparticles of high antibacterial potency against E. coli. Nanotechnology 23 (2012) 085103.
[61] Y. Liu, J. Padmanabhan, B. Cheung, J. Liu, Z. Chen, B.E. Scanley, D. Wesolowski, M. Pressley, C.C. Broadbridge, S. Altman, U.D. Schwarz, T.R. Kyriakides, J. Schroers, Combinatorial development of antibacterial Zr-Cu-Al-Ag thin film metallic glasses. Scientific Reports 6 (2016) 26950.
[62] J. Baker, S. Sitthisak, M. Sengupta, M. Johnson, R.K. Jayaswal, J.A. Morrissey, Copper stress induces a global stress response in Staphylococcus aureus and represses sae and agr expression and biofilm formation. Appl. Environ. Microbiol. 76 (2010) 150-160.

Graphical abstract

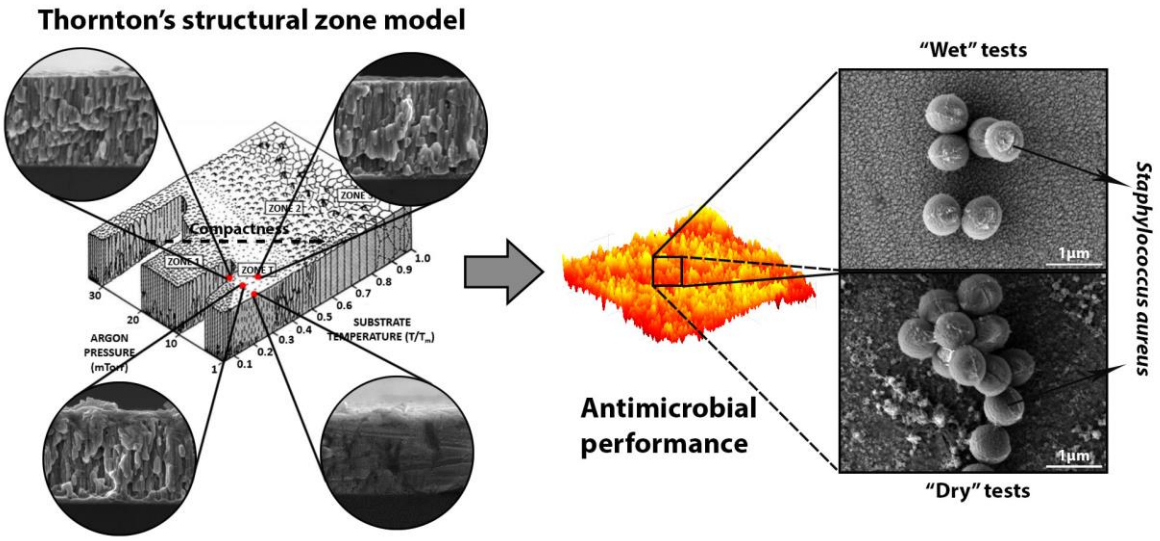

Highlights

- Thorton's model provides sensitive information to observe structural differences.
- Even within the same zone, differences in antimicrobial behaviour are detected.
- Low thin film compactness is required for high dry test antimicrobial performance.
- 4h dry contact on Cu-Zr thin films results in inner damage of *E. coli* and *S. aureus.*